



Research Article

ISSN : 0975-7384
CODEN(USA) : JCPRC5**Ligating, Spectral and Thermal Properties of Febuxostat Metal Complexes**Mamdouh S. Masoud¹, Alaa E. Ali^{2*}, Gehan S. Elasala² and Gomaa E. Amer²¹Chemistry Department, Faculty of Science, Alexandria University, Egypt²Chemistry Department, Faculty of Science, Damanshour University, Egypt**ABSTRACT**

Nine complexes of febuxostat with some transition metals [Cr(III), Mn(II), Fe(III), Co(II), Ni(II), Cu(II), Zn(II), Cd(II) and Hg(II)] were synthesized and discussed. The infrared spectra proved that febuxostat act as a bidentate ligand. The electronic spectra and magnetic measurements proved that all complexes have octahedral geometry except copper has trigonal bipyramidal geometry which confirmed by ESR. The thermal decomposition mechanisms of febuxostat and its metal complexes were studied and suggested from the DTA and TG curves. All complexes were thermally decomposed and ended by formation of the metal oxides except the complex of mercury.

Keywords: Febuxostat; Ligating; Complexes; Thermal analysis**INTRODUCTION**

Febuxostat is a urate lowering drug, a non-purine selective inhibitor of xanthine oxidase that is indicated for use in the treatment of hyperuricemia and chronic gout .It works by non-competitively blocking the molybdenum pterin center which is the active site on xanthine oxidase [1]. Febuxostat, chemically 2-[3-cyano-4-(2-methylpropoxy) phenyl]-4-methylthiazole-5-carboxylic acid [2].

Previous work for febuxostat metal complexes fell to synthesis of febuxostat complex with mercury in alkaline medium [3]. In this study the coordination properties of febuxostat metal complexes were discussed and identified by UV-Vis, IR, ESR and magnetic susceptibility measurements. The thermal behavior of febuxostat and its metal complexes were discussed from the TG and DTA curves. The proposed mechanism of decomposition is discussed. Also the thermodynamic and kinetic parameters were calculated.

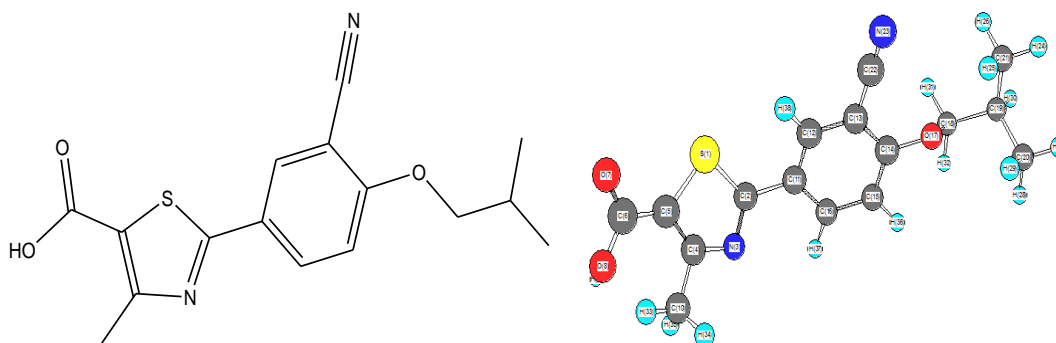


Figure 1 : Chemical Structure of Febuxostat (FBX)

EXPERIMENTAL SECTION

The solution of febuxostat was prepared by dissolving the solid in hot ethanol, while the solutions of the salts [Cr(III), Mn(II), Fe(III), Co(II), Ni(II), Cu(II), Zn(II), Cd(II) and Hg(II)] as chlorides were prepared by dissolving the salt in 50 ml bidistilled water. The solution of febuxostat was mixed with the aqueous solution of the metal chloride with molar ratio (1:1). The obtained precipitates were isolated by filtration, and then washed by EtOH-H₂O and dried in a vacuum desiccator over anhydrous CaCl₂. The analytical data, Table 1, of the prepared complexes examined by usual methods [4]. The chloride contents of the complexes were analyzed by using Volhard method [5]. Also the contents of metals were determined by using atomic absorption spectroscopy and complexometric analysis [6].

Measurements

The electronic spectra of the solid metal complexes were measured in Nujol mull spectra by use Unicam UV/Vis spectrometer [7]. The IR spectra of the febuxostat and its metal complexes were recorded on Perkin Elmer spectrophotometer, Model 1430 which it is range of 400-4000 cm⁻¹. The Molar magnetic susceptibilities were determined by using Pascal's constants at room temperature using Faraday's method. The electron spin resonance spectra were recorded on reflection spectrometer operating at (9.1–9.8) GHz in a cylindrical resonance cavity with 100 KHZ modulation. The values of g were determined by comparison with the standard DPPH signal. Differential thermal analysis and thermogravimetric analysis of the ligand and its complexes were recorded on Shimadzu DTA/TGA-60 thermal analyzer with heating rate 10°C/min under nitrogen atmosphere of flow rate 20 ml/min. Hyperchem computer program using PM3 semi-empirical and Molecular Mechanics Force Field (MM+) is applied for ligand.

Table 1: Elemental analysis, m.p. and color of febuxostat metal complexes

Complexes	Color	Calculated/(Found)%					
		C	H	N	S	M	Cl
[Cr(FBX)Cl ₂ (OH)H ₂ O]	Dark blue	40.52 (40.59)	4.04 (4.11)	5.91 (5.86)	6.76 (6.74)	10.96 (10.92)	14.95 (14.86)
[Mn(FBX) ₂ (H ₂ O) ₂]	Pale buff	53.25 (53.31)	4.75 (4.69)	7.76 (7.70)	8.89 (8.85)	7.61 (7.69)	-----
[Fe(FBX) ₂ ClH ₂ O]	Dark brown	51.93 (51.98)	4.36 (4.35)	7.57 (7.59)	8.67 (8.61)	7.55 (7.48)	4.79 (4.87)
[Co(FBX) ₂ (H ₂ O) ₂]	Faint pink	52.96 (52.88)	4.72 (4.78)	7.72 (7.71)	8.84 (8.79)	8.12 (8.09)	-----
[Ni(FBX) ₂ (OH) ₂]	Pale green	52.98 (53.01)	4.72 (4.65)	7.72 (7.78)	8.84 (8.82)	8.09 (8.13)	-----
[Cu(FBX)(OH)(H ₂ O) ₂]	Pale green	44.49 (44.53)	4.67 (4.68)	6.49 (6.56)	7.42 (7.46)	14.71 (14.67)	-----
[Zn(FBX)Cl(H ₂ O) ₃]	Pale yellow	40.87 (40.90)	4.50 (4.53)	5.96 (6.05)	6.82 (6.77)	13.91 (13.86)	7.54 (7.62)
Cd(FBX)Cl ₂ (H ₂ O) ₂ .H ₂ O	White	34.70 (34.67)	4.00 (3.98)	5.06 (4.98)	5.79 (5.86)	20.30 (20.39)	12.80 (12.72)
[Hg(FBX)(OH) ₂ (H ₂ O) ₂]	White	32.74 (32.68)	3.78 (3.81)	4.77 (4.69)	5.46 (5.39)	34.17 (34.20)	-----

The melting point of the all prepared complexes is higher than 300° C

RESULT AND DISCUSSION

The IR of febuxostat and its metal complexes are given in Table 2. Where febuxostat showed a broad band at 3172 cm⁻¹, Table 2, due to the νOH stretching of carboxylic group, the νC=O band of carboxylic group (COO) appears at 1676 cm⁻¹, and the band of νC-S appears at 1286 cm⁻¹. The band appears at 2233 cm⁻¹ represents νCN.

The bands at 1601-1689 cm⁻¹, corresponding to νC=O bands of the carboxylic group vibrations which are shifted in the spectra of all studied complexes indicating that the coordination occurred through that group. The νCN vibrational band is not changed for all studied complexes, where the cyanide group is not involved in coordination, so coordination occurred through the carboxylic group and the sulfur atom of thiazole ring, and febuxostat acts as a bidentate ligand forming a stable five membered ring with the metal ion. For all complexes, the broad bands in the range of 3403-3456 cm⁻¹ indicating of water in the

structure except for the complex $[\text{Ni}(\text{FBX})_2(\text{OH})_2]$, the broad band represents OH group. The shift of νCOO from 1676 to the range of 1601-1689 cm^{-1} for studied complexes indicates that coordination occurred by this group, the sulfur atom of thiazole ring is involved in coordination. The complex $[\text{Cr}(\text{FBX})\text{Cl}_2(\text{OH})\text{H}_2\text{O}]$ have broad band at 3456 cm^{-1} which represents water in the structure. The shift of νCOO from 1676 to 1688 cm^{-1} , Table 2, indicates coordination occurred through this group, the sulfur atom of thiazole ring is involved in coordination by shifting from 1286 to 1291 cm^{-1} and the ligand acts as a bidentate, the new bands at 577, 431 and 410 cm^{-1} , Table 2, represents $\nu\text{M-S}$ stretching, $\nu\text{M-O}$ stretching [8] and $\nu\text{M-Cl}$ respectively. Similar situations are evident for all the other complexes, Table 2. However, for Mn(II), Co(II), Ni(II), Cu(II) and Hg(II) complexes no peak appears for $\nu\text{M-Cl}$.

Table 2: Fundamental infrared bands of febuxostat (cm^{-1}) and its metal complexes

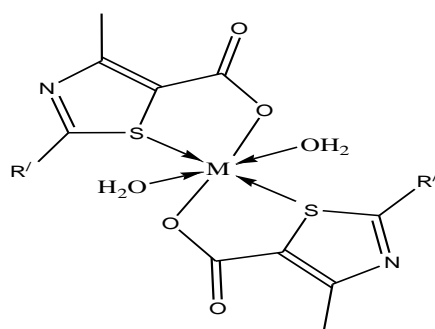
Compounds	νOH stretching	$\nu\text{C-S}$ stretching	νCOO stretching	$\nu\text{M-S}$	$\nu\text{M-O}$	$\nu\text{M-Cl}$
FBX	3172	1286	1676
$[\text{Cr}(\text{FBX})\text{Cl}_2(\text{OH})\text{H}_2\text{O}]$	3456	1291	1688	577	431	410
$[\text{Mn}(\text{FBX})_2(\text{H}_2\text{O})_2]$	3403	1292	1624	570	430
$[\text{Fe}(\text{FBX})_2\text{ClH}_2\text{O}]$	3424	1293	1614	595	455	415
$[\text{Co}(\text{FBX})_2(\text{H}_2\text{O})_2]$	3425	1292	1633	523	420
$[\text{Ni}(\text{FBX})_2(\text{OH})_2]$	3455	1291	1689	531	435
$[\text{Cu}(\text{FBX})\text{OH}(\text{H}_2\text{O})_2]$	3430	1292	1615	595	447
$[\text{Zn}(\text{FBX})\text{Cl}(\text{H}_2\text{O})_3]$	3403	1292	1601	546	461	425
$[\text{Cd}(\text{FBX})\text{Cl}_2(\text{H}_2\text{O})_2]\cdot\text{H}_2\text{O}$	3455	1291	1687	526	462	428
$[\text{Hg}(\text{FBX})\text{OH}(\text{H}_2\text{O})_2]$	3430	1292	1688	528	465

Electronic spectra and magnetic studies

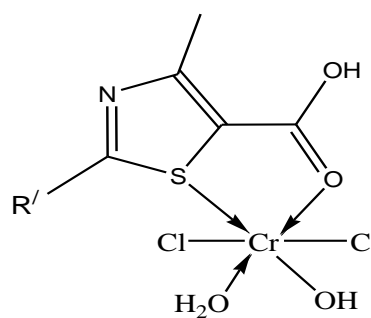
The electronic absorption spectra for the dark blue chromium $[\text{Cr}(\text{FBX})\text{Cl}_2(\text{OH})\text{H}_2\text{O}]$ complex showed three bands at 279, 425, 574 nm due to $4\text{A}_2\text{g} \rightarrow 4\text{T}_1\text{g}(\text{P})$, $4\text{A}_2\text{g} \rightarrow 4\text{T}_1\text{g}(\text{F})$ and $4\text{A}_2\text{g} \rightarrow 4\text{T}_2\text{g}(\text{F})$ transitions, respectively, Table 3. So the complex has octahedral geometry. Such octahedral geometry is deduced from the μ_{eff} value which equals, 4.95 B.M [9,10]. However, the electronic absorption spectra of the pale buff manganese complex, $[\text{Mn}(\text{FBX})_2(\text{H}_2\text{O})_2]$, Table 3, gave bands at 322, 399 and 450 nm where the first band is assigned to $6\text{A}_1\text{g} \rightarrow 4\text{A}_1\text{g}$, while the second is due to $6\text{A}_1\text{g} \rightarrow 4\text{T}_2\text{g}$ transition and the last band is due to $6\text{A}_1\text{g} \rightarrow 4\text{T}_1\text{g}$ transition [11,12]. Its room temperature μ_{eff} value of 5.94 B.M, typified the existence of Oh geometry. The electronic absorption spectra of dark brown iron complex, $[\text{Fe}(\text{FBX})_2\text{ClH}_2\text{O}]$, Table 3, gave bands at 319, 365, 450 nm. These bands are due to CT ($\text{t}_2\text{g} \rightarrow \pi^*$) and CT ($\pi \rightarrow \text{eg}$). Its room temperature μ_{eff} value of 5.77 B.M typified the existence of Oh configuration [13, 14]. The spectra for the faint pink $[\text{Co}(\text{FBX})_2(\text{H}_2\text{O})_2]$, Table 3, gave bands at 350, 415, 510 nm. The bands are of charge transfer, while the latter broad band is assigned to $4\text{T}_1\text{g}(\text{F}) \rightarrow 4\text{T}_1\text{g}(\text{P})$ transition with $\mu_{\text{eff}} = 4.52$ B.M typified the existence of octahedral geometry [15,16]. The pale green electronic absorption spectra for $[\text{Ni}(\text{FBX})_2(\text{OH})_2]$ showed three bands at 345, 415 and 700 nm due to $3\text{A}_2\text{g}(\text{F}) \rightarrow 3\text{T}_1\text{g}(\text{P})$ and $3\text{A}_2\text{g}(\text{F}) \rightarrow 3\text{T}_1\text{g}(\text{F})$ transitions, respectively, Table 3 with octahedral geometry, further deduced from the μ_{eff} value which equal 3.12 B.M. The pale green copper complex $[\text{Cu}(\text{FBX})\text{OH}(\text{H}_2\text{O})_2]$, Tables 3, exhibited bands at 390 and 760 nm, the data is harmony with trigonal bipyramidal geometry where the metal ion is five-coordinated with room temperature μ_{eff} value 1.78 B.M. The complexes of zinc, cadmium and mercury are diamagnetic with d^{10} configuration, so no d-d transition could be observed; the geometry of zinc, cadmium and mercury complexes was octahedral depending on elemental analysis.

Table 3: Nujol mull electronic absorption spectra λ max (nm), room temperature effective magnetic moment values (μ_{eff} , 298°K) and geometries of febusostat metal complexes.

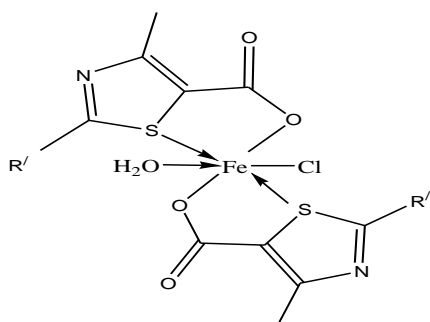
Complex	λ max (nm)	μ eff (B.M)	Geometry
[Cr(FBX)Cl ₂ (OH)H ₂ O]	279, 425, 574	4.95	Oh
[Mn(FBX) ₂ (H ₂ O) ₂]	322, 399, 450	5.94	Oh
[Fe(FBX) ₂ ClH ₂ O]	319, 365, 450	5.77	Oh
[Co(FBX) ₂ (H ₂ O) ₂]	350, 415, 510	4.52	Oh
[Ni(FBX) ₂ (OH) ₂]	345, 415, 700	3.12	Oh
[Cu(FBX)(OH)(H ₂ O) ₂]	390, 760	1.78	TBP
[Zn(FBX)Cl(H ₂ O) ₃]	Diamagnetic	Oh
[Cd(FBX)Cl ₂ (H ₂ O) ₂].H ₂ O	Diamagnetic	Oh
[Hg(FBX)(OH) ₂ (H ₂ O) ₂]	Diamagnetic	Oh



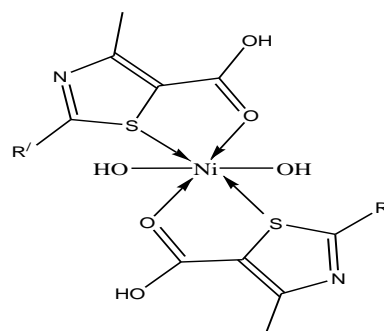
$R' = C_{11}H_{12}ON$
M= Mn(II), Co(II)



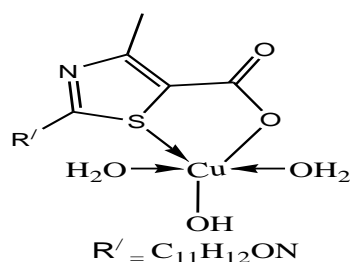
$R' = C_{11}H_{12}ON$
[Cr(FBX)Cl₂(OH)H₂O]



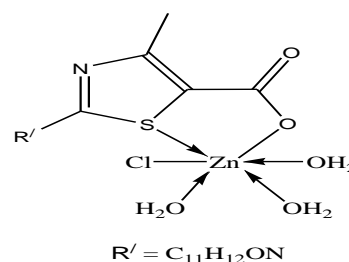
$R' = C_{11}H_{12}ON$
[Fe(FBX)₂ClH₂O]



$R' = C_{11}H_{12}ON$
[Ni(FBX)₂(OH)₂]



$R' = C_{11}H_{12}ON$
[Cu(FBX)(OH)(H₂O)₂]



$R' = C_{11}H_{12}ON$
[Zn(FBX)Cl(H₂O)₃]

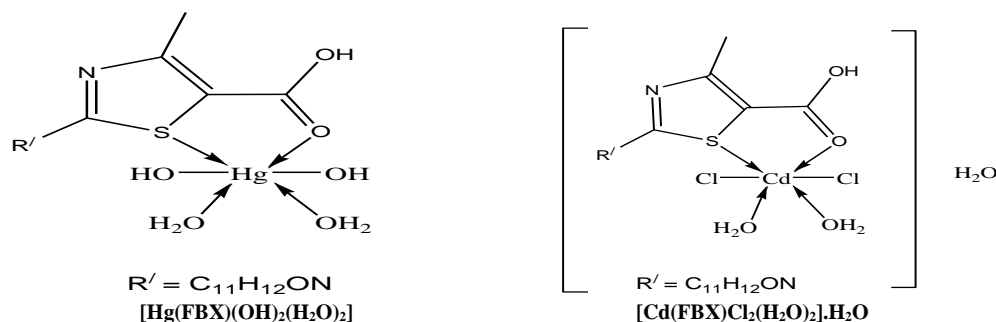


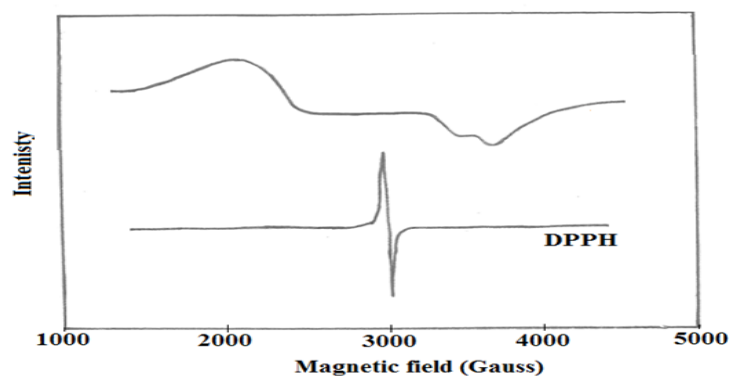
Figure 2: Proposed structures of febusostat metal complexes

Electron spin resonance of copper complex

The ESR spectrum of the trigonal bipyramidal $[Cu(FBX)(OH)(H_2O)_2]$ complex, Figure 3 and Table 4, showed anisotropic spectrum of an axial-compressed type. It gave two g values, $g_{//} = 2.045$, $g_{\perp} = 2.223$. The calculated $\langle g \rangle$ value; $\langle g \rangle = (g_{//} + 2g_{\perp})/3$ was 2.163. When $g_{\perp} > g_{//}$ suggests that dZ^2 ground state is present [17]. However, the low value of f_2 of the complex indicates a strong axial field.

Table 4 : Room temperature ESR spectral parameters of copper febusostat complex

complex	g_{\perp}	$g_{//}$	$\langle g \rangle$	$104A_{//}$	$104A_{\perp}$	$104\langle A \rangle$	G	f_2	α^2
$[Cu(FBX)(OH)(H_2O)_2]$	2.223	2.045	2.163	265	45	118	0.197	0.802	0.913

Figure 3: X-band ESR spectra of $[Cu(FBX)(OH)(H_2O)_2]$ complex.**Thermal analysis**

The thermal analysis of some coordination compounds has been reported from Masoud *et al* [18-22]. The study of thermal analysis of febusostat (Figure 10) and its metal complexes were investigated. In this study different techniques were used: thermogravimetric analysis (TGA) and differential thermal analysis (DTA). The data of analysis are collected in Table 5. In case of the free ligand (febusostat), the decomposition occurred in two steps, Figure 4. The first step of decomposition started above 30 °C, the weight loss was 8.85% due to the loss of ethylene molecule. The step accompanied by the endothermic effect in the DTA curve at temperature 84°C, this step ended at 125.2°C. The second step of decomposition started above 196°C and the weight loss was 88.13%, this step ended at 600°C and accompanied by the exothermic effect in the DTA curve at temperature 395.8°C. All TGA steps were ended by carbon residue with 3.31%. The suggested mechanism of decomposition is given in Figure 5.

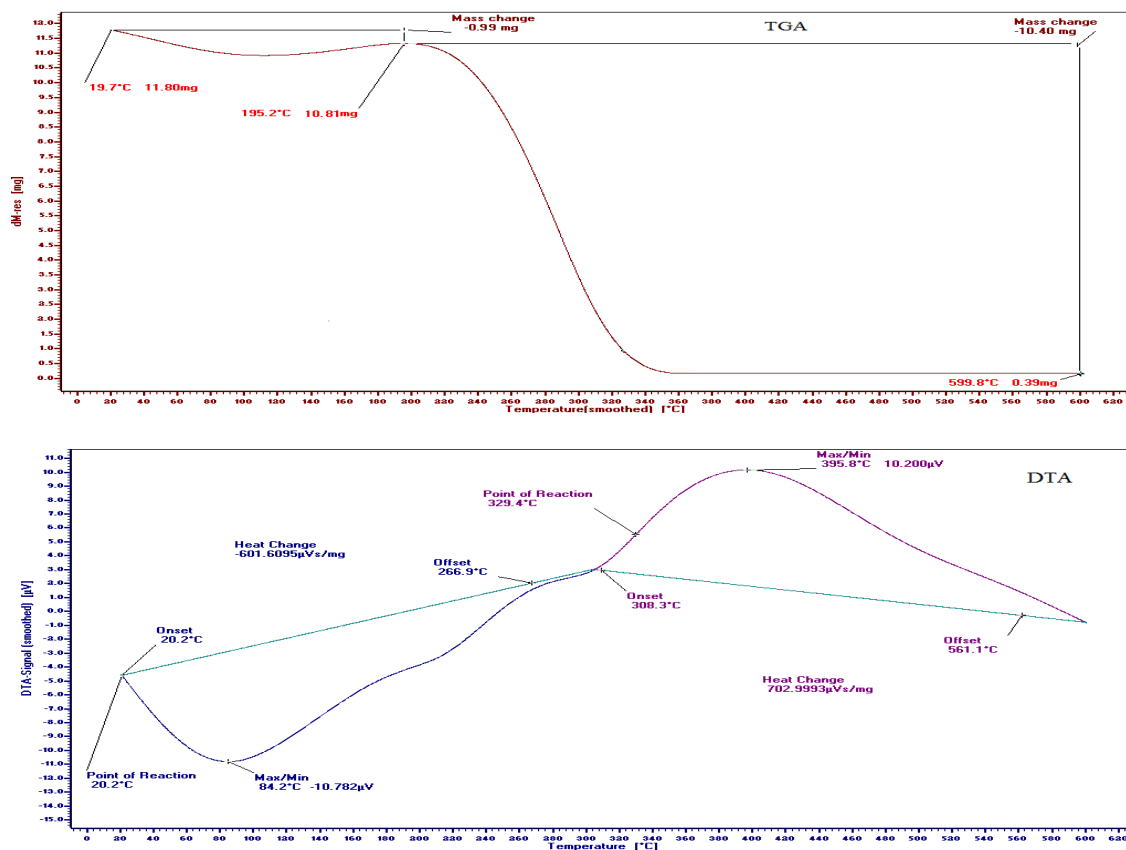


Figure 4: TGA and DTA curves for febusostat

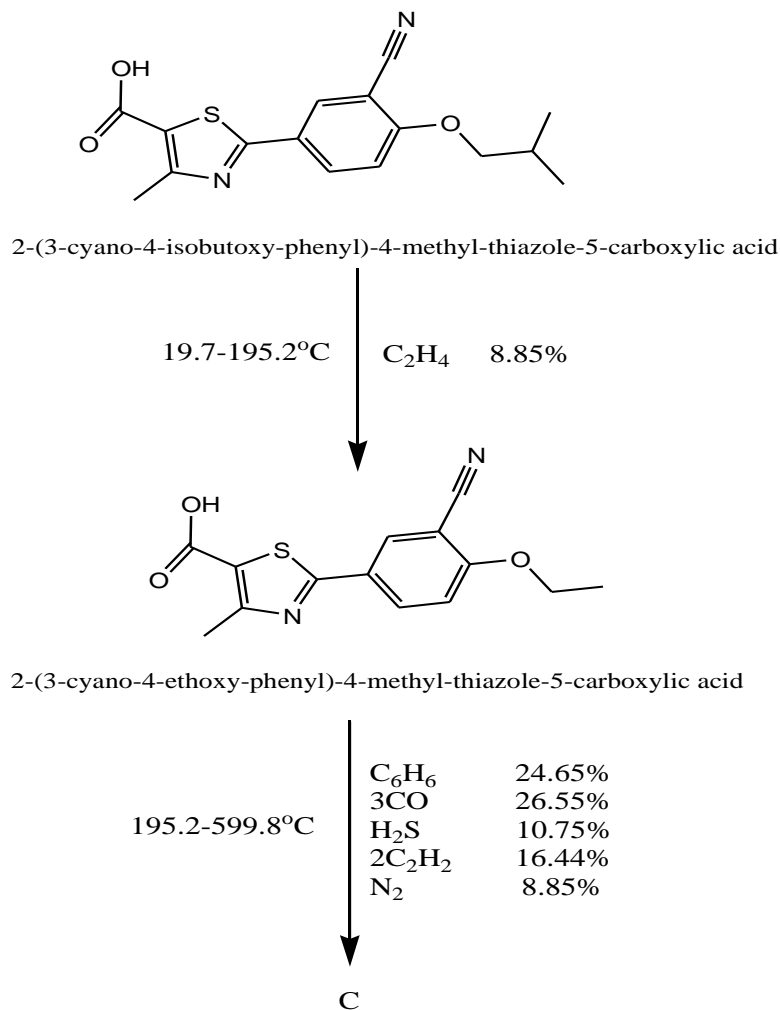
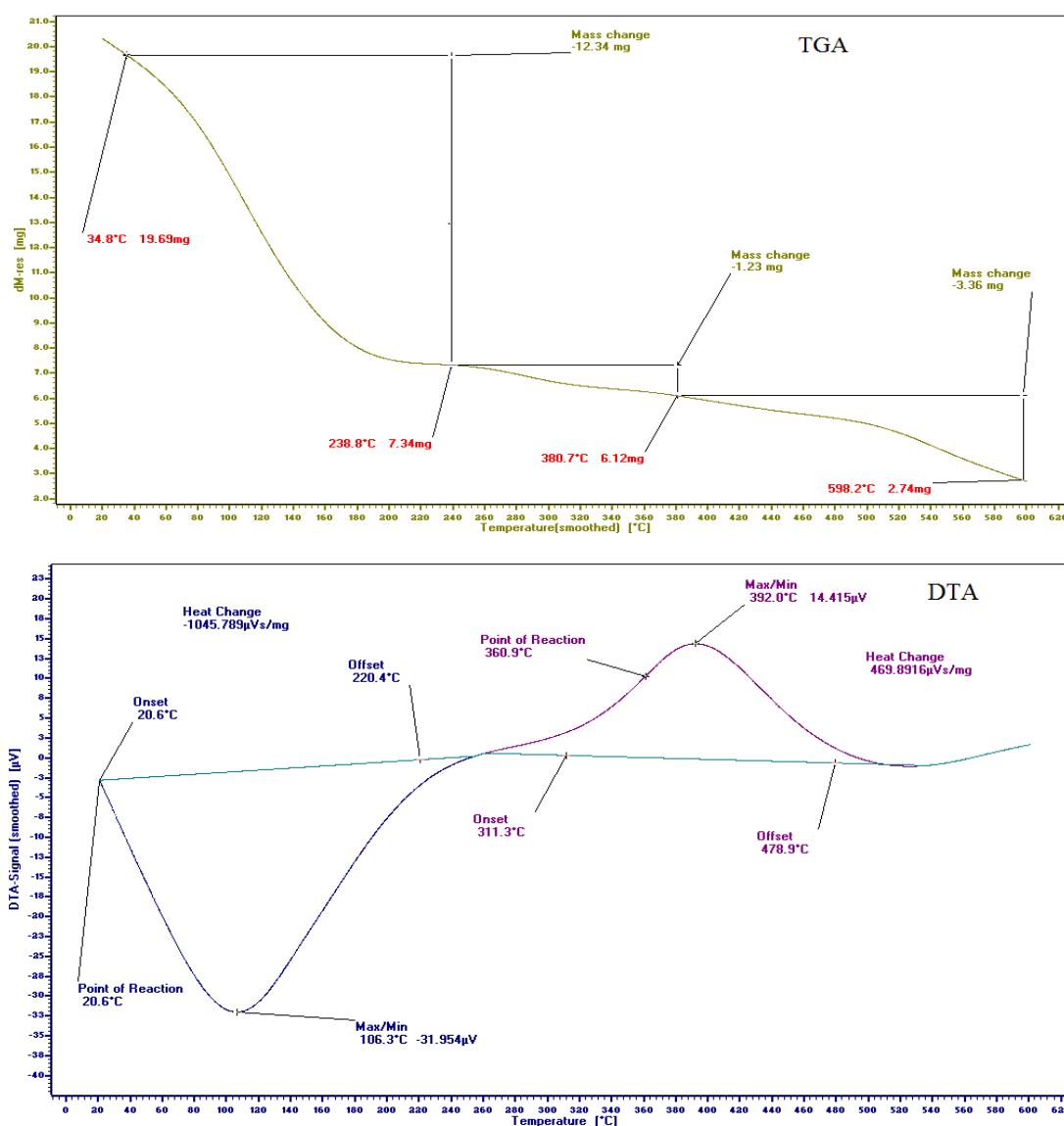


Figure 5: Suggested mechanism of decomposition of febuxostat

The $[\text{Co}(\text{FBX})_2(\text{H}_2\text{O})_2]$ complex, Figure 6, was decomposed in three steps, the first step of decomposition started at 35°C, the weight loss was 62.67% and ended at 238.8°C which accompanied by the endothermic effect in the DTA curve at temperature 106.3°C. The second step of decomposition started above 240 °C and the weight loss was 6.25% due to the loss of acetylene molecule, this step ended at 380.7°C. While the last step was in temperature range between 390-598.2°C, and the weight loss was 17.06%. The second and the last steps in TGA are overlapped to give an exothermic peak in DTA thermogram which appeared in temperature range 260-540°C. The three TGA peaks are due to decomposition steps of the complex which ended with the formation of CoO and 2C as a final product. The suggested mechanism of decomposition is given in Figure 7.

**Figure 6: TGA and DTA curves for $[\text{Co}(\text{FBX})_2(\text{H}_2\text{O})_2]$ complex**

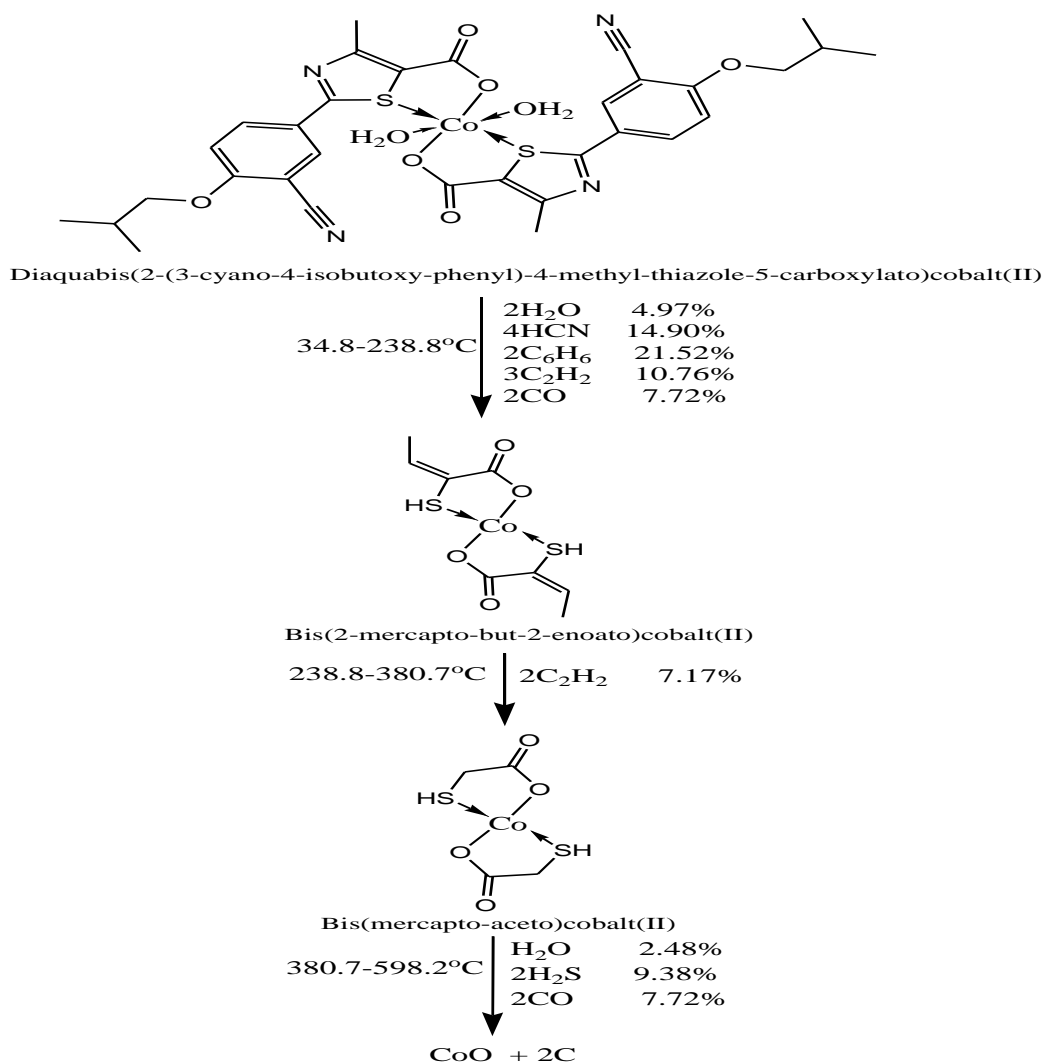


Figure 7 : Suggested mechanism of decomposition of [Co(FBX)2(H2O)2] complex

For the [Ni(FBX)2(OH)2] complex, Figure 8, the thermal decomposition occurred in three steps, the first step of decomposition started at 40.8°C, the weight loss was 58.24% and ended at 205.3°C which accompanied by the endothermic effect in the DTA curve at temperature 102.5°C. The second step of decomposition started above 206 °C and the weight loss was 10.59%. The step ended at 430.3°C. The third step decomposed above 431°C, and the weight loss was 15.10% and ended at 591.6°C. The second and the third steps in TGA are overlapped to give an exothermic peak in DTA thermogram which appeared in temperature range 235.5-600°C. The three TGA steps are due to decomposition of the complex which ended with the formation of NiO and 3C as a final product, the complexes of cobalt and nickel was taken as example for illustration of thermal behavior of febuxostat complexes. The suggested mechanism of decomposition is given in Figure 9.

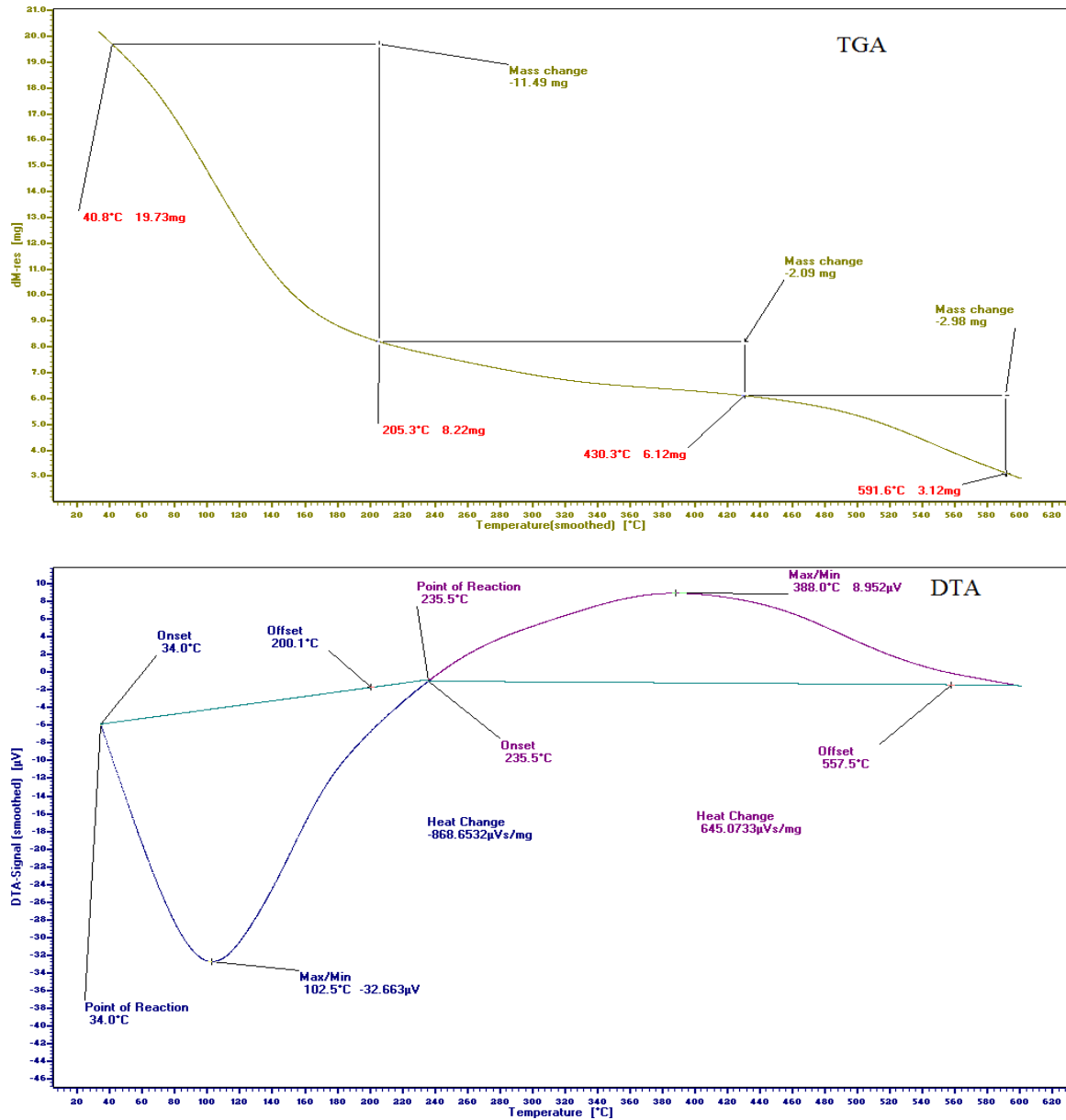
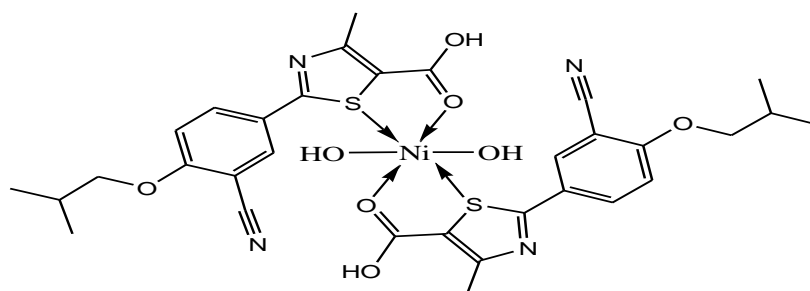


Figure 8: TGA and DTA curves for [Ni(FBX)2(OH)2] complex



Dihydroxobis((2-(3-cyano-4-isobutoxy-phenyl)-4-methyl-thiazole-5-carboxylic acid))nickel(II)

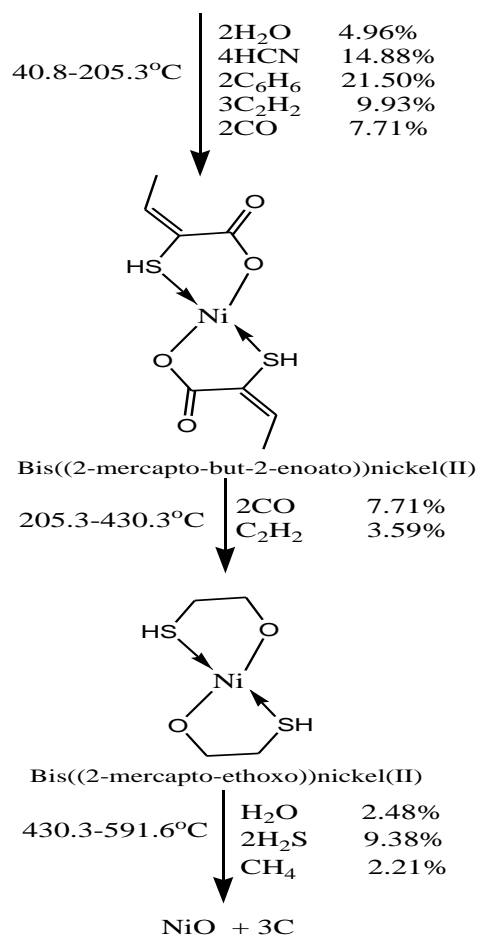
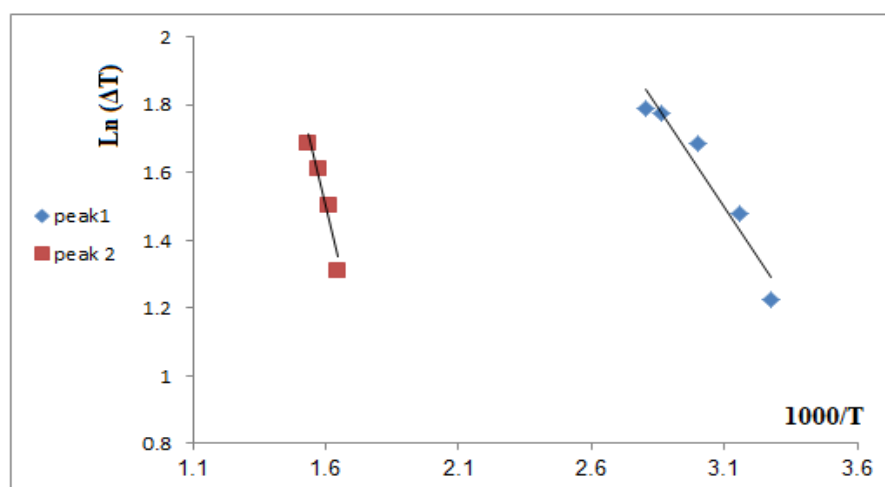
Figure 9: Suggested mechanism of decomposition of [Ni(FBX)₂(OH)₂] complexFigure 10: lnAT against 10³/T relation for febusostat ligand (as a representative figure)

Table 5 : DTA analysis of febuxostat and its metal complexes

Compound	Type	T _m (°K)	E _a kJ mol ⁻¹	n	α _m	ΔS [#] kJ K ⁻¹ mol ⁻¹	ΔH [#] kJ mol ⁻¹	Z S ⁻¹	Temp. (°C) TGA	Wt. Loss %		Assignment
										Calc	Found	
Febuxostat	Endo	357	9.72	1.44	0.56	-0.313	-111.786	0.003	19.7-195.2	8.85	8.39	Elimination of C ₂ H ₄ .
	Exo	669	21.53	1.58	0.55	-0.317	-212.046	0.033	195.2-599.8	87.24	88.13	Loss of C ₆ H ₆ , 3CO, N ₂ , 2C ₂ H ₂ and H ₂ S, forming C as residue.
[Cr(FBX)Cl ₂ (OH)H ₂ O]	Endo	368	20.00	1.28	0.59	-0.308	-113.209	0.007	33.7-122.2 122.2-285.2	48.53 19.1	50.67 19.91	Loss of H ₂ O, 2HCN, C ₆ H ₆ , 2C ₂ H ₂ and CO. loss of CO, HCl and C ₂ H ₂ .
	Exo	676	57.48	1.28	0.59	-0.309	-208.861	0.010	159.8-322.1	27.61	26.61	Elimination of the rest of ligand, forming 0.5Cr ₂ O ₃ .
[Mn(FBX) ₂ (H ₂ O) ₂]	Endo	363.4	21.37	1.13	0.61	-0.307	-111.518	0.007	40.2-166.9	41.82	43.18	Loss of 2H ₂ O, 2HCN, 6C ₂ H ₂ , and 2CO.
	Exo	804.7	27.19	1.38	0.57	-0.318	-255.967	0.004	166.9-367.0 367.0-599.9	18.53 19.64	18.27 18.87	Loss of 2HCN, 2C ₂ H ₂ and C ₂ H ₄ Decomposition of the rest of ligand, forming MnO+6C.
[Fe(FBX) ₂ ClH ₂ O]	Endo	361	14.66	1.29	0.58	-0.310	-111.873	0.005	34.5-227.8	45.37	44.09	Elimination of H ₂ O, 2HCN, 2C ₆ H ₆ , 2C ₂ H ₂ and 2CO.
	Exo	741	26.58	1.16	0.60	-0.317	-234.827	0.004	227.8-431.1 431.1-597.9	7.56 23.16	6.87 22.27	Elimination of 2C ₂ H ₄ . Decomposition of the rest of ligand, forming 0.5Fe ₂ O ₃ +8C.
[Co(FBX) ₂ (H ₂ O) ₂]	Endo	379	13.86	1.34	0.58	-0.311	-117.934	0.004	34.8-238.8	59.87	62.67	Elimination of 2H ₂ O, 4HCN, 2C ₆ H ₆ , 3C ₂ H ₂ and 2CO.
	Exo	665	49.61	1.26	0.59	-0.309	-206.096	0.009	238.8-380.7 380.7-598.2	7.17 19.58	6.25 17.06	Loss of 2C ₂ H ₂ . Elimination of the rest of ligand, forming CoO+2C.

Compound	Type	T _m (°K)	E _a kJ mol ⁻¹	n	α _m	ΔS [#] kJ K ⁻¹ mol ⁻¹	ΔH [#] kJ mol ⁻¹	Z S ⁻¹	Temp. (°C) TGA	Wt. Loss %		Assignment
										Calc	Found	
[Ni(FBX) ₂ (OH) ₂]	Endo	376	17.84	1.39	0.57	-0.309	-116.161	0.006	40.8-205.3	58.98	58.24	Loss of 2H ₂ O, 4HCN, 2C ₆ H ₆ , 3C ₂ H ₂ and 2CO.
	Exo	699	17.02	1.33	0.58	-0.319	-223.428	0.003	205.3-430.3 430.3-591.6	11.30 14.07	10.59 15.10	Loss of 2CO and C ₂ H ₂ . Decomposition of the rest of ligand, forming NiO+3C.
[Cu(FBX)OH(H ₂ O) ₂]	Endo	365	15.91	1.31	0.58	-0.309	-112.93	0.005	33.0-161.6	45.14	46.03	Loss of 2H ₂ O, HCN, C ₆ H ₆ , C ₂ H ₂ and CO.
	Exo	690	24.27	1.46	0.56	-0.316	-218.368	0.004	161.6-291.9 291.9-600.0	15.28 18.01	15.51 16.88	Loss of 2C ₂ H ₂ and 0.5N ₂ . Elimination of the rest of ligand, forming CuO+C.
[Zn(FBX)Cl(H ₂ O) ₃]	Endo	377	12.70	1.46	0.56	-0.312	-117.552	0.004	36.2-215.0	17.44	17.43	Loss of 3H ₂ O and CH ₂ CH ₂ .
	Exo	756	141.23	1.51	0.55	-0.303	-229.335	0.022	215.0-380.0 380.0-596.3	39.57 26.06	39.81 26.22	Loss of 2HCN, C ₆ H ₆ , C ₂ H ₂ , CO Decomposition of the rest of ligand, forming ZnO.
[Cd(FBX)Cl ₂ (H ₂ O) ₂]. H ₂ O	Endo	382	8.10	1.12	0.61	-0.316	-120.623	0.003	32.2-206.6	9.76	10.57	Loss of 3H ₂ O.
	Exo	636	22.30	1.52	0.55	-0.316	-200.864	0.004	206.6-543.5 543.5-698.2	24.00 42.96	23.66 42.96	Loss of HCN, 3C ₂ H ₂ , CO. Decomposition of the rest of ligand, forming CdO.
[Hg(FBX)(OH) ₂ (H ₂ O) ₂]	Endo	368	10.29	1.46	0.56	-0.313	-115.242	0.003	35.4-153.7	6.13	6.69	Elimination of 2H ₂ O.
	Exo	699	10.70	1.02	0.63	-0.324	-226.125	0.002	153.7-306.7 306.7-599.7	76.94 14.82	76.54 14.01	Loss of HCN, CH ₃ COOH, Hg, H ₂ CO, 2CO and C ₆ H ₆ . Elimination of the rest of ligand, forming carbon residue.

CONCLUSION

The complexes of febuxostat was synthesized and characterized by different spectroscopic methods. The stoichiometry of complexes was determined by the analytical data. All complexes have octahedral geometries except copper complex has trigonal bipyramidal geometry. The Nujol mull electronic spectra confirmed these results. An ESR spectrum of copper complex was studied. The spectral data confirmed that febuxostat acts as a bidentate ligand. The kinetic and thermodynamic parameters were calculated from the differential thermal analysis curves. All complexes were thermally decomposed and ended by formation of metal oxides except the complex of mercury.

REFERENCES

- [1] Love BL; Barrons R; Veverka A; Snider KM. *Pharmacotherapy*. **2010**, 30(6), 594-608
- [2] Savjani K; Gajjar A; Savjani J. *Int J of Pharm and Pharm Sci*. **2016**, 8(1), 359-366.
- [3] Somasekhar G; Mamatha P; Rani SN; Kumar NR; Zabiullah SI; Basha MM. *Int J of Chem and Pharm Sci*. **2016**, 4(8), 434-438
- [4] Vogel AI. *A Text Book of Quantitative Inorganic Analysis*, Longmans, London. **1989**.
- [5] Lee RH; Griswold E; Kleinberg. *J Inorg Chem*. **1964**, 3, 1278-1283
- [6] Schwarzenbach G. *Complexometric Titration*, Translated by H, Methuen Co., London, Irving. **1957**.
- [7] Mohamed GB; Masoud MS; Hindawy AM; Ahmed RH. *J Pharm Sci*. **1989**, 3(2), 141-145.
- [8] Price ER; Wasson JR. *J Inorg Nucl Chem*. **1974**, 36 (1) 711-716.
- [9] Howlader MBH; Islam MS; Karim MR. *J Chem*. **2000**, 39, 407-409.
- [10] Sreekanth A; Joseph M; Fun HK; Kurup MRP. *Polyhedron*. **2006**, 25(6), 1408-1414.
- [11] Buhl F; Sroka BS. *Chem Anal*. **2003**, 48, 58-145.
- [12] Barefield DW. *J Inorg Nucl Chem*. **1961**, 22, 3-4.
- [13] Barnum DW. *J Inorg Nucl Chem*. **1961**, 22(4), 183-191.
- [14] Lever ABP. Elsevier publish Co, Amsterdam, **1968**.
- [15] Barefield EK; Busch DH; Nelson SM. *Quart Rev*. **1968**, 22(4), 457- 498.
- [16] Masoud MS; Zaki ZM. *Transition Met Chem*. **1988**, 13(5), 321-327
- [17] Garribba E; Micera G. *J of Chem Edu*. **2006**, 83(8), 1229.
- [18] Masoud MS; Ali AE; Ahmed HM; Mohamed EA. *J Mol Str*. **2013**, 1050, 43-52.
- [19] Masoud MS; Ali AE; Elasala GS. *Spectrochim. Acta A*. **2015**, 149, 363-377.
- [20] Masoud MS; Ali AE; Ghareeb DA; Nasr NM. *J Mol Str*. **2015**, 1099, 359-372.
- [21] Masoud MS; Ali AE; Elasala GS; Kolkaila AS. *J chem pharm Res*. **2017**, 9(4), 171-179.
- [22] Masoud MS; Ali AE; Elasala GS; Kolkaila AS. *Spectrochim. Acta A* **2018**, 193, 458-466